# Leveraging SUMO for Real-World Traffic Optimization: A Comprehensive Approach

Olga Dobrilko[1] Alon Bublil[2]

April 25, 2024

**Abstract**

This paper illuminates the utilization of SUMO as a powerful tool for addressing real-world traffic management issues. There is a gap in testing and validating solutions to in-field conditions due to the high cost and complexity of urban and suburban road networks. The validation step is often skipped, which can lead to a higher risk in implementing sophisticated solutions that exist in our multimodal transportation environment. This challenge is addressed by introducing simulations as a crucial preliminary step before real-world application. Accurate simulations require detailed data on intersection geometries, vehicle distribution, and driver behavior to accurately mirror real-world conditions. To meet these criteria, detailed sensor data on trajectories, types of road users, and their locations are extensively employed. This data forms the foundation for calibrated traffic simulations by NoTraffic™ . In conclusion, an in-depth demonstration of the method used to address a real-world traffic problem with SUMO is provided, emphasizing SUMO's effectiveness in building confidence for deploying solutions in the field.

**Keywords:** SUMO, ATSPMs, Calibration, Traffic Management, Traffic Optimization

## 1 Introduction

Addressing the complexities of managing traffic in dense urban areas presents a significant challenge that necessitates innovative solutions and strategies. As a real-time traffic management platform, our focus lies in preventing traffic congestion and improving the overall traffic efficiency [1].

To efficiently solve issues and reduce frictions we need the ability to test our approaches before deploying them in the field. Currently, many agencies implement new solutions and configurations directly on-site, a process that inherently creates issues as the effects of the changes being deployed cannot be accurately predicted. To mitigate these challenges, some agencies adopt testing methods such as Synchro [2] and NetSim [3].

These methods, useful for establishing basic timing plans and provide base-level splits, cycles, and offsets, are not precise enough for real-time optimization, which requires microscopic simulation. This simulation allows us to model traffic flows based on the motion of each individual vehicle, including acceleration, deceleration, and lane changes for each driver. Examples of microscopic

[1]Sr. Automation Engineer at NoTraffic™ , olga@notraffic.tech , orcid: 0009-0000-1174-8899
[2]Algorithm Tech Lead at NoTraffic™ , alon@notraffic.tech , orcid: 0009-0002-4243-4491

traffic flow simulators include Aimsum, VISSIM, MITSIMLab, DRACULA and of course SUMO [4][5].
We have observed that in many simulations, discrepancies arise because the geometry does not closely align with the real world or the distribution of vehicles is not representative. These limitations prevent the complete reproduction of field issues in simulations. Overcoming this gap is an essential aspect when addressing real-world problems.

In the following sections, more details are given on the rich data provided by NoTraffic™ and demonstrate how we fully leverage it to construct a realistic simulation that tackles the above-mentioned challenges. A calibrated model allows us to bridge the gap between the field and simulation.
This approach enables us to adopt a 'simulate-before-deploy' strategy. When presented with a solution to an issue, we aim to test it across diverse scenarios to evaluate its impact on the system as a whole. This approach enables us to build confidence in our solution before deploying it in the field.

# 2 Terminology

## 2.1 NoTraffic™ Data

The NoTraffic™ Sensor Units collect data on each road user (object) through fused video and radar detection. A Sensor Unit is installed at every approach, ensuring a comprehensive perspective of traffic at the intersection. Data from the Sensor Units is sampled at

$$f > 1\,\mathrm{Hz} \tag{1}$$

yielding a robust and extensive dataset that is used for real-time signal timing optimization and data analytics.

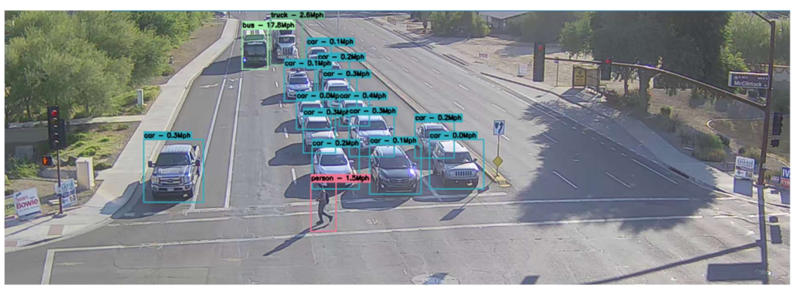

**Sensor Unit field of view, showing data for each road user**

Figure 1: Road users detection

The Sensor Units collect the following data for each road user:

1. Classification: car, bus, truck, motorcycle, pedestrian, bicycle, light rail.
2. Position: lane, phase, distance from stop bar, direction, speed.

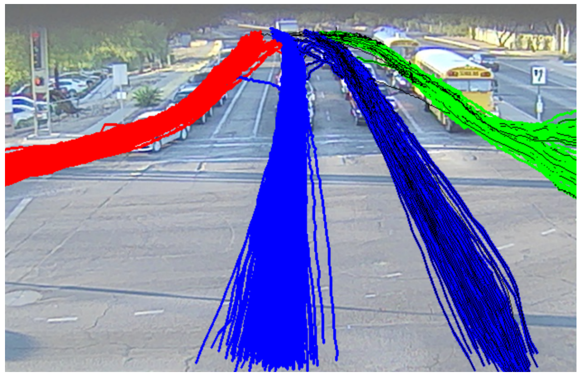

Figure 2: Trajectories per lane.

Additionally, the NoTraffic™ system also provides trajectories for each lane.
All sensor data is securely transmitted and stored in the cloud.

### 2.2 Traffic Management

When examining the effectiveness of traffic signals in ensuring efficiency and productivity, it's crucial to consider the following factors contributing to their effectiveness:

1. Safety - provide safe transportation for all roadway users.
2. Efficiency - minimize delays, congestion and effective approach management.

To manage traffic effectively within the constraints of safety and efficiency, a control strategy must be developed, usually this is done using signal timing plans [6] [7].
The design of such a control strategy has significantly impacts the performance of urban traffic systems. Current traffic signal plans involve complex control logic and a multitude of parameters that require configuration.

However, in real-world applications of timing plans, there is typically no established practice of thorough and continuous evaluation. Simulation-based signal optimization has been limited, mainly due to the heavy computational burden associated with it [8].

### 2.3 Signal Performance Measures

Automated Traffic Signal Performance Measures (ATSPMs) have garnered significant attention for their capability to collect and assess real-time and historical data at signalized intersections. ATSPM data is widely utilized by traffic engineers, planners, and researchers in various applications scenarios [9] [10].

This paper discusses some of the common ATSPM datasets used by NoTraffic™ :

### 2.3.1 Traffic counts

This fundamental metric captures the number of vehicles that cross during a given time period, denoted as $T$. This count can be conducted for all approaches collectively or individually.

Let $N$ represent the total count during time period $T$. From this, the flow rate $v$ can be derived using the formula:

$$v = \frac{N}{T} \tag{2}$$

Usually, $T$ is set to 15 minutes, but more accurate flow rates can be obtained by using smaller time intervals, such as minutes or seconds.

### 2.3.2 Average delay per vehicle

An important measure of effectiveness (MOE) at a signalized intersection is delay, which can be classified into several types [11].
Here, we focus on stopped delay, which accounts for periods when vehicles are stationary within a specific time frame $T$. The equation used in this context is given as:

$$d = \frac{1}{N} \sum_{i=1}^{N} \{t \mid s_{r_i t} < 3_{m/s}\} \tag{3}$$

where,
$N$ = number of vehicles
$s_{r_i t}$ = speed of the vehicle $r_i$ at time $t$, for $t \in T$.

### 2.3.3 Arrival on Green - AoG

AoG is a metric indicating phase progression, approximating the ratio of vehicles arriving when the traffic light is green versus the total number of vehicles arriving within the time frame $T$. A good measure of progression is when vehicles arrive at the intersection on green and can proceed smoothly without needing to stop.

$$AoG = \frac{N_g}{N} \tag{4}$$

where $N_g$ = number of vehicles arrived on green.
$N$ = total number of vehicles arrived at the intersection for all $t \in T$.

### 2.3.4 Split Failure

A split failure occurs when a phase $p$ turns red while there is still a queue [12].
Split failure is an important aspect of ATSPM, minimizing incidents of split failures indicates adequate service for all approaches.

## 3 Realistic Micro-Simulation in SUMO

To accurately replicate real-world traffic conditions, a highly precise micro-simulation must be developed. Several key steps are involved in creating a realistic simulation. Firstly, it's essential to create a SUMO network that closely resembles real-world road layouts. Next, the integration of actual traffic light control systems is crucial for reproducing real-world traffic management. Thirdly, scenarios based on data from real-world situations need to be created. Finally, the simulation undergoes calibration to accurately replicate real-world traffic. Methodologies for each stage of traffic modeling, based on real- world data, will be discussed in further detail in a later section.

### 3.1 SUMO Network

Creating a SUMO network for urban intersections can be complex. While Open Street Maps (OSM) data is commonly used, it often contains inaccuracies such as incorrect number of lanes, directions, and traffic light setup. These errors can result in an unrealistic SUMO network that is unsuitable for accurate traffic simulations. Figure 3 illustrates these issues, including misplaced traffic lights and mismatched lane details, compared to the actual intersection layout.

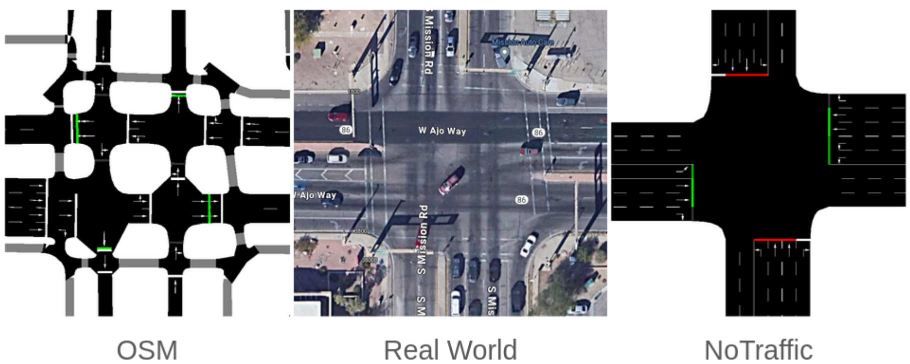


Figure 3: Intersection layout: OSM, Real-World, NoTraffic™ generated intersection.

Relying solely on OSM may not be adequate to accurately create city intersection layouts [13]. Incorporating additional data sources like Google Earth/Maps or paid services can enhance network generation, aiming for a simple yet accurate intersection representation (see Figure 3). The NoTraffic™ System addresses this by generating necessary data during installation and configuration, which is then uploaded to the cloud. This data includes intersections locations (lat, lon), trajectories and lanes including bike lanes and left/right turn lanes pockets lengths.

This data, which includes number of lanes and trajectories for each entry point, aids in the creation of network edges and connections using a specialized tool for generating networks. An example of an intersection layout derived from this data is illustrated in Figure 4.

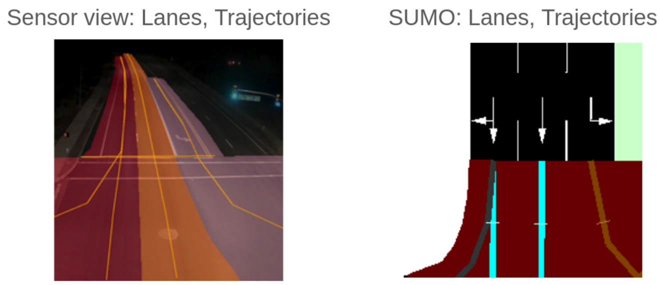


Figure 4: SUMO network approach edge and connections generated from NoTraffic™ cloud data.

### 3.2 Traffic Light Controllers

To accurately simulate real-world scenarios, mirroring actual traffic light operations at intersections is crucial. In addition to using SUMO, a customized traffic light controller block has been developed. This block can be tailored to replicate the specific traffic light setup of a real intersection, with additional data sourced from the NoTraffic™ cloud, including lane phase mapping and detector data.
The integration process involves:

- Configuring software-in-the-loop (SIL) controllers to match actual field controllers.
- Mapping SUMO network traffic light link indexes to corresponding controller phases.
- Adding lane mappings to detectors.

The virtual controller is a SIL type ring-based controller. Our API supports the integration of multiple types of SIL into the simulation. Compared to the builtin SUMO NEMA-controller [14], it incorporates advanced features such as overlaps and controller logic statements. These enhancements enable a more precise replication of traffic light controllers within simulations. The simulation process, incorporating these controllers at each simulation step, is presented in the following figure:

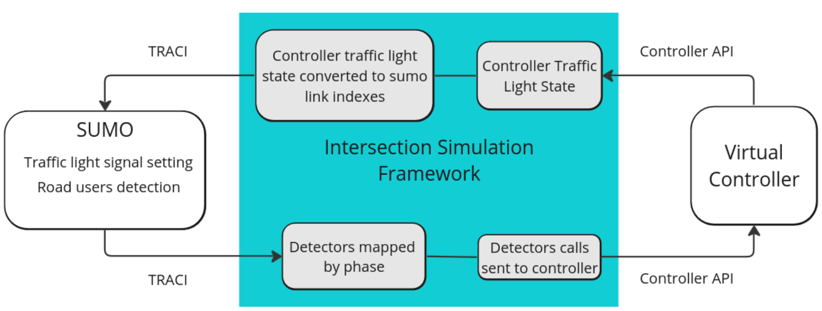


Figure 5: SIL Framework.

### 3.3 Simulation Scenario

Often, simulations used by traffic practitioners lack accurate and up-to-date real-world traffic counts. When such data is available, it typically represents total vehicle counts for only a part of the day. Additionally, the data may lack precise details about the types of road users: car, bus, bicycle, motorcycle, truck, emergency vehicle, pedestrian, light rail and tram. For creating a representative traffic scenario, a precise distribution of these counts and their types is crucial.
NoTraffic™ sensors detect road users in every lane and classify them according to the types mentioned above. All of the data is uploaded to the cloud at a resolution of 1 second.
This data is employed to identify platoons, which are groups of road users progressing together. These platoons are then inserted into the simulation.
The significance of accurate platoon distribution is illustrated in Figure 6. The figure compares the flow of road users in scenarios using accurately distributed platoons versus uniformly distributed platoons based on total counts. There is a noticeable difference in the flow rate between the two, significantly impacting the simulation outcome. The figure presents the distinction of road user platoons in scenarios using high-resolution platoons versus uniformly distributed count-based platoons.

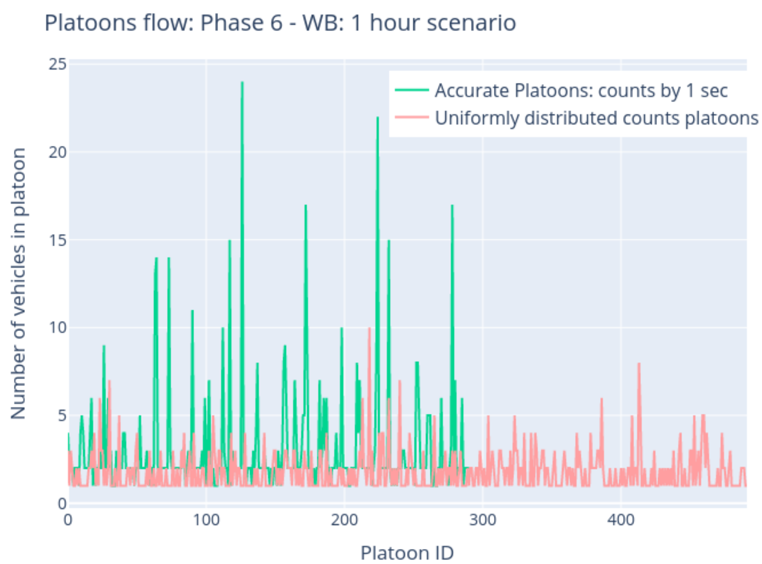


Figure 6: Platoons method vs uniformly distributed counts.

Simulation users can retrieve data for any hour and date, converting it into a format suitable for SUMO. This capability is made possible by a tool integrated within the simulation, which allows for the immediate execution of scenarios for the requested time periods.
The process for executing a scenario is as follows: Vehicle distribution data is pulled from the cloud and undergoes several manipulations, resulting in:

- Route assignment to each vehicle
- Time of insertion assignment for each vehicle

- Vehicle type assignment (e.g., bus, passenger car, bike)

This processed data is then saved to a file and subsequently uploaded into the simulation. Each step, the simulation fetches and inserts vehicles for that time step using SUMO's add() method, which includes the relevant route and vehicle type. Vehicles are inserted at the end position of the source edge of their route in the network.
This procedure may contain some inaccuracies, which will be identified and addressed in future enhancements.

## 3.4 Calibration

Calibration is an essential step for enhancing the accuracy of the simulation. The more accurate the simulation, the easier it is to replicate real-world behavior, and it aids in accurately predicting the impact of improvements. To achieve accurate results, several factors need to be taken into consideration:

- Metrics for calibration.
- Car-Following model selection.
- Input parameters for calibration.
- Calibration method.

The selection of the appropriate car following model for use will be addressed in future research. The current model we are working with is Weidemann 99 [15].

### 3.4.1 Calibration metrics

Calibration metrics include ATSPMs such as counts, Arrival on Green(AoG), and average delays. A standard parameter for calibration is speed [16][17], which is highly correlated with average delay and AoG (refer to sections 2.3.2 and 2.3.3). The count metric ensures that all anticipated road users are included in the simulation. Metrics derived from the simulation are then compared with those collected in the field, which are stored in the cloud. ATSPMs are adopted as calibration metrics, aligning with traffic engineers who depend on these performance indicators for field-based traffic operation assessments.

### 3.4.2 Car-following model

Several car-following models were evaluated, including Krauss, IDM, and Weidemann 99. To avoid overfitting, the models were tested across over 20 intersections and different scenarios. The Weidemann 99 model was selected as the most suitable based on its superior calibration performance at most intersections. The calibration utilized similar input parameters across models, although the Weidemann model had a distinct parameter, CC2, which was set to default value (refer to section 3.4.3). A comparison of the calibration results for the average delay ATSPM metric among the Krauss, Weidemann 99, and IDM models is provided in a Figure 7. Although the results were comparable, only the Weidemann 99 model met the absolute error threshold of 5 seconds for average delay per phase.

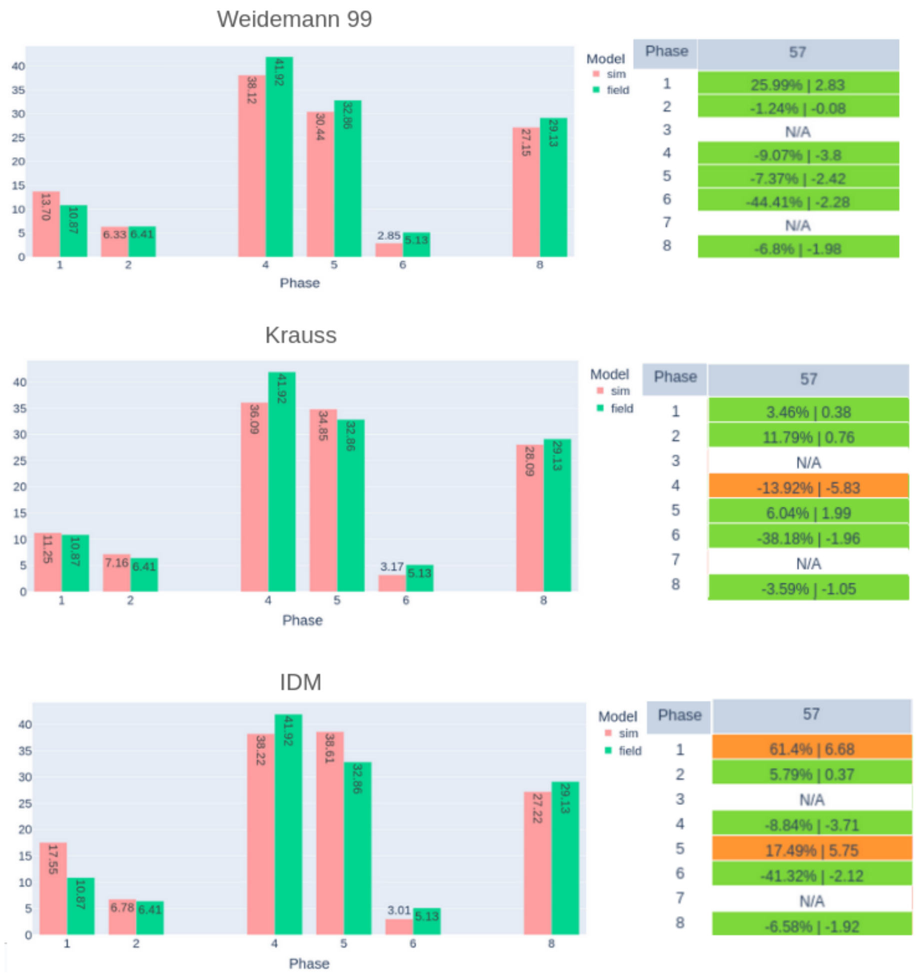


Figure 7: Krauss, IDM, W99 calibration results compare: average delay per phase.

The Weidemann 99 model includes unique thresholds that impact driver behavior [18]. An example from field observations is the varying following distance between vehicles over time. The CC2 parameter addresses this behavior. Further investigation is needed into the unique parameters of the Weidemann 99 model and their effects on driver behavior in simulations. Likewise, the distinctive parameters of other models should be explored. Therefore, additional research into car-following models in SUMO will be conducted.

### 3.4.3 Calibration input parameters

Input parameters for calibration are presented in the table below. Some parameters are unique to Weidemann 99 such as thresholds defining drivers behavior [15]. A unique parameter that is used in calibration is CC2, which represents following distance variation [m]:

Table 1: Calibration input parameters.

| Parameter | Default Value | Lower Bound | Upper Bound | Description |
|---|---|---|---|---|
| CC1 | 1.2 s | 0.5 s | 2.5 s | Desired headway time between lead/prioritized and following vehicles. |
| CC2 | 8 m | 1 m | 10 m | Following variation. |
| CC8 | $2.0\,\mathrm{m/s^2}$ | $0.5\,\mathrm{m/s^2}$ | $5.0\,\mathrm{m/s^2}$ | Standstill acceleration. |
| minGap | 2.5 m | 0.5 m | 5 m | Empty space after leader. |
| desiredMaxSpeed | varies by road user | 1.39 m/s | 50 m/s | Road user speed by type. |
| startupDelay | 0 s | 0 s | 3 s | Delay time before starting to drive after having had to stop. |
| jmDriveAfterYellowTime | -1 s | -1 s | 5 s | Violation yellow light if the light has changed more recently than the given threshold. |

The calibration process is designed to calibrate passenger cars, as they represent approximately 95% of road users. In future studies, additional types of road users will be considered.

#### 3.4.4 Calibration method

The calibration approach involves executing a comprehensive grid search to explore all feasible combinations of parameter values within a pre-defined range. Achieving perfect alignment between simulated outcomes and actual field measurements without any deviation is an unattainable goal in our domain. To mitigate this, we employ the Chi-square statistical method to compute the error for each metric in each phase, given by:

$$\chi^2 = \sum_{p=1}^{n} \frac{(O_p - E_p)^2}{E_p} \tag{5}$$

Where:
$O_p$ = scaled observed metric in simulation averaged over the entire scenario period per phase
$E_p$ = scaled expected metric in field averaged over the entire scenario period per phase
$p$ = phase

Each metric is characterized by a unique scale: counts are approximately $10^3$, average delay spans from $10^{-1}$ to $10^2$, and Arrival on Green range from 1 to $10^2$. For the purpose of computing the overall error, it is essential to normalize these metrics. The method used for scaling is a variation of MinMaxScaler per phase:

$$E_p = \frac{e_p}{M - m}, O_p = \frac{o_p}{M - m} \tag{6}$$

Where:
$o_p$ = unscaled observed metric in simulation averaged over the entire scenario period per phase
$e_p$ = unscaled expected metric in field averaged over the entire scenario period per phase
$M$ = Maximum metric value per phase
$m$ = minimum metric value per phase

Each metric is calculated as mentioned in section 2.3. Delay and Arrival on Green are computed and averaged for each phase over the entire scenario period. Prior to consolidating these averages for the entire scenario, each cycle is evaluated to ensure it is representative for inclusion in the overall average. Specifically, Z-Score Method and Minimum Size Threshold were used to filter statistical outliers. Counts are computed as total counts of vehicles over all approaches.

The total error is the sum of all the metric errors, weighted equally:

$$error = \frac{1}{3} \cdot \sqrt{\chi^2_{total.count}} + \frac{1}{3} \cdot \sqrt{\sum_{p=1}^{n} \chi^2_{avg.delay(p)}} + \frac{1}{3} \cdot \sqrt{\sum_{p=1}^{n} \chi^2_{AoG(p)}} \tag{7}$$

Hence, among all input parameters permutations, the one with the minimum error is selected. In addition to achieving minimal error, the error for each metric must comply with specific percentage and absolute thresholds for maximum allowable error. Further details will be discussed in future work. The simulation undergoes calibration for peak hour scenarios, which historically exhibit the highest level of saturation. Input parameters that yield the minimum error and meet the specified thresholds are selected to run simulations for further research.

### 3.4.5 Calibration results

Our calibration method is demonstrated on one of NoTraffic™ 's intersection, denoted by I57. The calibration results in terms of ATSPMs are displayed below. Metrics calculated in simulation are compared to metrics obtained from the field.
The calibration used a scenario from PM peak hours, resulting the following optimal parameters:

Table 2: Optimal parameters.

| **Parameter** | **Value** |
|---|---|
| CC1 | 1.2 s |
| CC2 | 4 m |
| CC8 | $2.5\,\mathrm{m/s^2}$ |
| minGap | 1.4 m |
| desiredMaxSpeed | 17.89 m/s |
| startupDelay | 0 s |
| jmDriveAfterYellowTime | 1 s |

This setup yields the following results for our calibration metrics for average delay, counts and Arrival on Green presented accordingly in the figure below:


Figure 8: Calibration results: Average Delay, Counts and Arrival on Green.

It can be noted that the simulation results do not perfectly reflect field conditions. Achieving zero error is impractical due to the large number of variables that influence drivers behavior in the real world. Errors in counts can often be attributed to vehicles at the end of the scenario not entering the sensor range at intersections, where their detection is possible. This occurs because vehicles are inserted in the end of route source edge. Consequently, further enhancements are required in the insertion of scenario vehicles as discussed in 3.3. Therefore, a maximum error threshold is permissible, with errors in counts allowed up to 8%. Beyond this percentage, the flow of vehicles would represent a different scenario. Additionally, the discrepancies in other calibrated metrics may be explained by equal values of calibrated input parameters across all lanes and intersections in the network. Future efforts will focus on lane-specific speed calibration.

# 4 Real world application of SUMO

As a company specializing in traffic optimization across multiple urban areas, NoTraffic™ occasionally encounters the need to address on-site challenges, resolving and testing them prior to deployment. Recently, NoTraffic™ addressed a citizen complaint in one of the major agencies we are collaborating with.

The issue observed in the Eastbound Left Turn (EBLT), phase 5, involves recurrent split failures during the PM peak.
This left turn phase experiences significant demand during the peak, as demonstrated by the following counts. As you can see, EBLT is the busiest left turn approach.

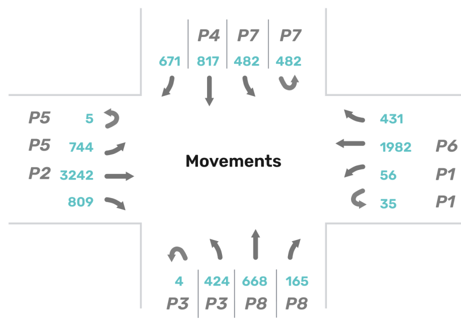


Figure 9: Counts by approach.

The queue was building during several cycles causing a spillback to the through movement lane.

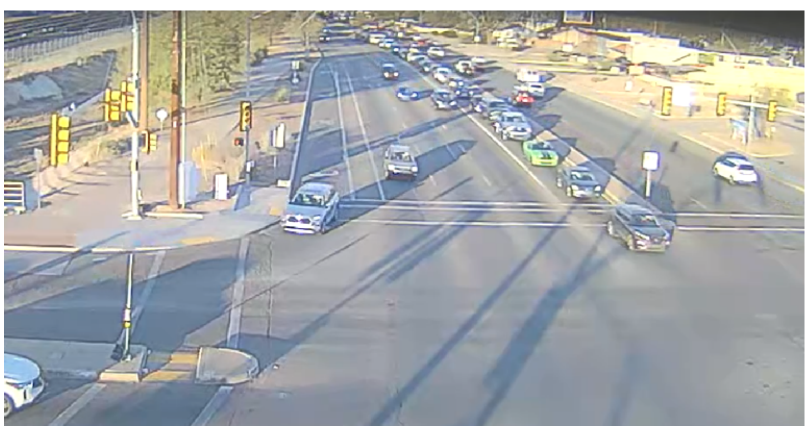

Figure 10: Split failure of EBLT in the field.

This case study illustrates the importance of proper calibration when using SUMO models to address real-world traffic issues.

In the initial step of our solution, SUMO plays a key role. We leverage its capabilities to replicate the issue by simulating the intersection scenario at the time of the incident. This allows us to visually identify the problem before proceeding with resolution efforts.

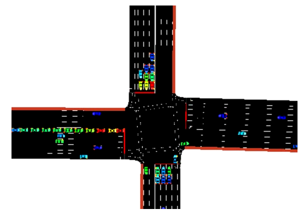

Figure 11: Split failure of phase 5 - EBLT.

Once the spillback was successfully reproduced in simulation, several strategies were tested in our algorithm.

The one we chose to use is called ”flush queue”, an ability we developed in NoTraffic™ . The ”flush queue” strategy is designed to improve the existing ”gap out” behavior of controllers. By leveraging detailed data on queue length, estimated time of arrival (ETA) for each vehicle, and vehicle type, as well as queue information from other approaches, we can develop a more intelligent and adaptable strategy. This approach allows for the continued servicing of a phase as long as there is still a significant queue. Following the implementation of the flush queue strategy, conducting another simulation yields significant improvements as shown in figure 12.

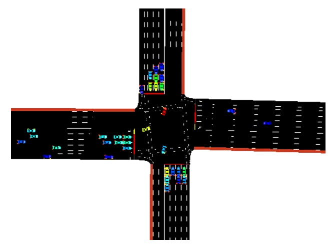

Figure 12: Split failure of EBLT after flush queue.

While we observed that the issue was solved for that specific time by examining the SUMO video, we want to ensure its stability throughout the entire day. After examining the data for a full hour, it becomes clear that the improvement remains consistent throughout, with a notable 50% enhancement, as illustrated in the figure below.

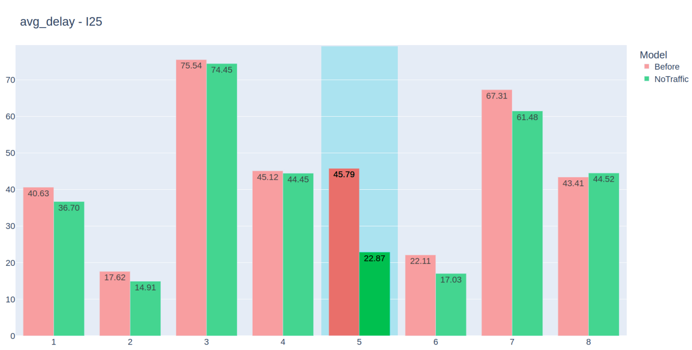


Figure 13: Comparison of delay of phase 5.

Once we confirm that the issue is solved in the simulation, we can confidently deploy the change in field and monitor its behavior. In our analysis, we observed a 43% improvement in the average delay of phase 5 after deploying our fix.


Figure 14: Avg. delay of EBLT in field: before vs. after flush queue.

It's noteworthy that in simulations, there was a 50% improvement, whereas in the field, the improvement was 43%. This discrepancy can be attributed to various factors: the day measured after implementing the solution does not entirely match the day simulated. Additionally, the simulation may need further calibration. Despite these variations, achieving such similar values is a significant achievement, underscoring the strong correlation between the simulation and real-world outcomes.

This section highlights NoTraffic™ 's application of SUMO in resolving real-world traffic issues in an urban area. Focused on addressing a specific traffic congestion problem identified through citizen feedback, the section outlines the steps taken from problem identification to solution deployment. By leveraging SUMO's simulation capabilities, NoTraffic™ was able to replicate the issue, test various strategies, and implement a solution that significantly improved traffic flow, demonstrating a practical approach to urban traffic management using simulation.

# 5 Conclusion

This paper has demonstrated the practical application of SUMO in tackling real-world traffic optimization challenges. By leveraging the rich data provided by NoTraffic™ sensors, we have showcased the ability to create realistic traffic simulations through precise calibration. By reproducing real-world scenarios and testing various strategies in simulation, such as the "flush queue" strategy highlighted in our case study, we can confidently deploy solutions that improve traffic flow and reduce congestion in urban areas. In future work we will provide more details on our calibration process and how we accurately generate vehicle distributions for scenarios to match those observed in the field.

### Data availability statement

The data is not publicly accessible due to its ownership by a private corporation.

### Competing interests

The authors declare that they have no competing interests.

### CRediT authorship contribution statement

**Olga Dobrilko:** Conceptualization, Methodology, Software, Validation, Formal Analysis, Writing - Review & Editing.
**Alon Bublil:** Conceptualization, Methodology, Software, Validation, Formal Analysis, Writing - Review & Editing.

## References


[1] Aleksandar Stevanovic and Milan Zlatkovic. Evaluation of insync adaptive traffic signal control in microsimulation environment. In *92nd Annual Meeting of the Transportation Research Board, Washington DC*, 2013.

[2] Kijawattanee Udomsilp, Teeratat Arayakarnkul, Sorawee Watarakitpaisarn, Patrachart Komolkiti, Jittichai Rudjanakanoknad, and Chaodit Aswakul. Traffic data analysis on sathorn road with synchro optimization and traffic simulation. DOI: 10.4186/ej.2017.21.6.57, 2017.

[3] J Shadewald and Clyde Prem. Quantifying access management benefits using traffic simulation. In *Proceeds of the Ninth TRB Conference on the Application of Transportation Planning Methods*, pages 187–196, 2003.

[4] Jesus Felez, Joaquin Maroto, Jose M Cabanellas, and Jose M Mera. A full-scale simulation model to reproduce urban traffic in real conditions in driving simulators. DOI: 10.1177/0037549713483557, 2013.

[5] Pablo Alvarez Lopez, Michael Behrisch, Laura Bieker-Walz, Jakob Erdmann, Yun-Pang Flötteröd, Robert Hilbrich, Leonhard Lücken, Johannes Rummel, Peter Wagner, and Evamarie Wießner. Microscopic traffic simulation using sumo. Available online: `https://elib.dlr.de/127994/`, 2018.

[6] Peter Koonce and Lee Rodegerdts. Traffic signal timing manual. Available online: `https://nacto.org/docs/usdg/signal_timing_manual_fhwa.pdf`, 2008.

[7] Halim Ceylan and Michael GH Bell. Traffic signal timing optimisation based on genetic algorithm approach, including drivers' routing. DOI: 10.1016/S0191-2615(03)00015-8, 2004.

[8] Tamir Balasha and Tomer Toledo. Simulation-based optimization of actuated traffic signal plans. Available online: `https://transp-or.epfl.ch/heart/2014/abstracts/051.pdf`, 2015.

[9] Bangyu Wang, Grant G Schultz, Gregory S Macfarlane, Dennis L Eggett, and Matthew C Davis. A methodology to detect traffic data anomalies in automated traffic signal performance measures. DOI: 10.3390/futuretransp3040064, 2023.

[10] Bangyu Wang, Grant G Schultz, Gregory S Macfarlane, and Sabrina McCuen. Evaluating signal systems using automated traffic signal performance measures. DOI: 10.3390/futuretransp2030036, 2022.

[11] Ali Payidar Akgungor and A Graham R Bullen. Analytical delay models for signalized intersections. Available online: `https://nacto.org/docs/usdg/analytical_delay_models_for_signalized_intersections_akgungor.pdf`, 1999.

[12] Federal Highway Administration. Automated traffic signal performance measures. Available online: `https://ops.fhwa.dot.gov/publications/fhwahop20002/fhwahop20002.pdf`, 2020.

[13] Christian Bewermeyer, Rüdiger Berndt, Sebastian Schellenberg, Reinhard German, and David Eckhoff. Poster: cosmetic-towards reliable osm to sumo network conversion. Available online: `https://www.david-eckhoff.net/pdf/bewermeyer2015cosmetic.pdf`, 2015.

[14] Max Schrader, Qichao Wang, and Joshua Bittle. Extension and validation of nema-style dual-ring controller in sumo. DOI: 10.52825/scp.v3i.115, 2022.

[15] Bryan Higgs, Montasir Abbas, and Alejandra Medina. Analysis of the wiedemann car following model over different speeds using naturalistic data. Available online: `https://onlinepubs.trb.org/onlinepubs/conferences/2011/RSS/3/Higgs,B.pdf`, 2011.

[16] Bawan Mahmood and Jalil Kianfar. Driver behavior models for heavy vehicles and passenger cars at a work zone. DOI: 10.3390/su11216007, 2019.

[17] Biagio Ciuffo, Vincenzo Punzo, Marcello Montanino, et al. The calibration of traffic simulation models: Report on the assessment of different goodness of fit measures and optimization algorithms multitude project–cost action tu0903. DOI: 10.2788/7975, 2012.

[18] Bryan Higgs, Montasir Abbas, and Alejandra Medina. Analysis of the wiedemann car following model over different speeds using naturalistic data. Available online: `https://onlinepubs.trb.org/onlinepubs/conferences/2011/RSS/3/Higgs,B.pdf`, 2011.